

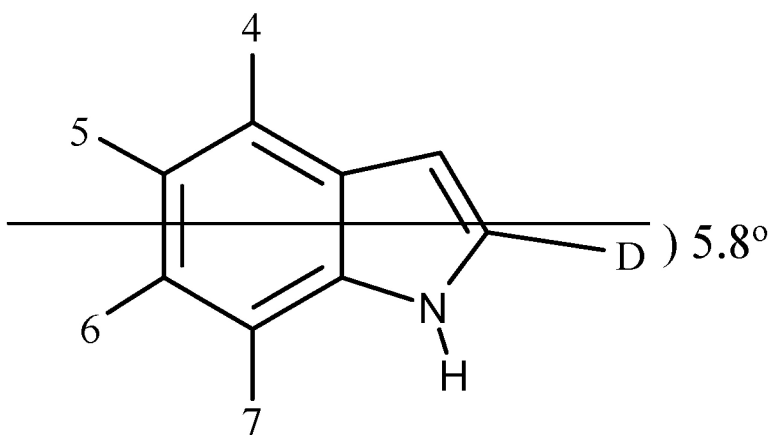
Article

## Combined Experimental/Theoretical Refinement of Indole Ring Geometry Using Deuterium Magnetic Resonance and *ab Initio* Calculations

Koeppe, Haiyan Sun, Patrick C. A. van der Wel, Erin M. Scherer, Peter Pulay, and Denise V. Greathouse

*J. Am. Chem. Soc.*, **2003**, 125 (40), 12268-12276 • DOI: 10.1021/ja035052d • Publication Date (Web): 11 September 2003

Downloaded from <http://pubs.acs.org> on March 29, 2009



### More About This Article

Additional resources and features associated with this article are available within the HTML version:

- Supporting Information
- Links to the 3 articles that cite this article, as of the time of this article download
- Access to high resolution figures
- Links to articles and content related to this article
- Copyright permission to reproduce figures and/or text from this article

[View the Full Text HTML](#)

## Combined Experimental/Theoretical Refinement of Indole Ring Geometry Using Deuterium Magnetic Resonance and *ab Initio* Calculations

Roger E. Koeppe, II,\* Haiyan Sun, Patrick C. A. van der Wel, Erin M. Scherer, Peter Pulay, and Denise V. Greathouse

*Contribution from the Department of Chemistry and Biochemistry, University of Arkansas, Fayetteville, Arkansas 72701*

Received March 7, 2003; E-mail: rk2@uark.edu.

**Abstract:** We have used experimental deuterium NMR spectra from labeled tryptophans in membrane-spanning gramicidin A (gA)<sup>1</sup> channels to refine the geometry of the indole ring and, specifically, the C2–<sup>2</sup>H bond direction. By using partial exchange in a cold organic acid, we were able to selectively deuterate ring positions C2 and C5 and, thereby, define unambiguous spectral assignments. In a backbone-independent analysis, the assigned spectra from four distinct labeled tryptophans were used to assess the geometry of the planar indole ring. We found that the C2–<sup>2</sup>H bond makes an angle of about 6° with respect to the normal to the indole ring bridge, and the experimental geometry was confirmed by density functional calculations using a 6-311G\*\* basis set. The precisely determined ring geometry and the experimental spectra in turn are the foundation for calculations of the orientation of each tryptophan indole ring, with respect to the bilayer membrane normal, and of a principal order parameter *S*<sub>zz</sub> for each ring. The results have general significance for revising the tryptophan ring geometry that is used in protein molecular modeling, as well as for the analysis of tryptophan ring orientations in membrane-spanning proteins. The experimental precision in the definition of the indole ring geometry demonstrates yet another practical application emanating from fundamental research on the robust gramicidin channel.

### Introduction

Deuterium magnetic resonance spectroscopy using solid or liquid-crystalline oriented samples is a powerful tool for local structure analysis.<sup>2,3</sup> For example, specific alanine labels have served to define not only the magnitude and direction of tilt of a membrane-spanning  $\alpha$ -helix but also the geometry of the alanine side chain in  $\alpha$ -helices (which is incorrect in some standard libraries).<sup>4</sup> Similar uncertainties surrounding the indole ring geometry have hampered solid-state NMR investigations of tryptophans in membrane proteins.<sup>5,6</sup> Certainly, protein molecular modeling and structural refinement methods depend critically upon libraries with accurate geometries for the individual amino acids. In this paper, we report a refinement of the indole ring geometry of Trp side chains; and, we confirm experimental predictions using *ab initio* calculations. In addition to calculations, our methods involve the use of solid-state

deuterium NMR spectroscopy, applied to oriented samples of a membrane-spanning peptide. The results hold general significance for protein structure modeling.

As opposed to soluble proteins which may tumble freely, a membrane protein is expected to assume a preferred directional orientation with respect to a bilayer membrane normal.<sup>4</sup> Indeed, the fluid-mosaic model<sup>7</sup> allows membrane proteins to diffuse and rotate at defined levels within the bilayer, yet restricts them firmly to the bilayer plane and permits little translation along the bilayer normal, and little rotation that would change their orientations with respect to the bilayer normal. An “anchoring” relative to the bilayer normal is accomplished through specific interactions at the interface, typically using either charged residues<sup>8,9</sup> or aromatic tyrosines and tryptophans.<sup>10–12</sup> For example, a striking WWFW sequence occurs at one of the putative membrane/water interfaces in the human cellular receptor for anthrax toxin.<sup>13</sup> For the case of membrane-spanning gramicidin (gA)<sup>1</sup> channels, opposing subunits are anchored

- (1) Abbreviations: DMPC, dimyristoylphosphatidylcholine; Fmoc, 9-fluorenylmethoxycarbonyl; gA, gramicidin A; QCC, quadrupolar coupling constant; rmsd, root-mean-square deviation; SDS, sodium dodecyl sulfate; *S*<sub>zz</sub>, principal order parameter about the long molecular axis (the helix axis) of the gramicidin channel;<sup>31</sup> *V*<sub>zz</sub>, principal “on-bond” component of the electric field gradient tensor.
- (2) Davis, J. H.; Auger, M. *Prog. Nucl. Magn. Reson. Spectrosc.* **1999**, *35*, 1–84.
- (3) Opella, S. J.; Marassi, F. M. *Methods Enzymol.* **2001**, *339*, 285–313.
- (4) Van der Wel, P. C. A.; Strandberg, E.; Killian, J. A.; Koeppe, R. E., II. *Biophys. J.* **2002**, *83*, 1479–1488.
- (5) Koeppe, R. E., II; Hatchett, J.; Jude, A. R.; Providence, L. L.; Andersen, O. S.; Greathouse, D. V. *Biochemistry* **2000**, *39*, 2235–2242.
- (6) Grage, S. L.; Wang, J.; Cross, T. A.; Ulrich, A. S. *Biophys. J.* **2002**, *83*, 3336–3350.

- (7) Singer, S. J.; Nicolson, G. L. *Science* **1972**, *175*, 720–731.
- (8) Von Heijne, G. *EMBO J.* **1986**, *5*, 3021–3027.
- (9) De Planque, M. R. R.; Kruijtzter, J. A.; Liskamp, R. M.; Marsh, D.; Greathouse, D. V.; Koeppe, R. E., II; de Kruijff, B.; Killian, J. A. *J. Biol. Chem.* **1999**, *274*, 20839–20846.
- (10) Schiffer, M.; Chang, C. H.; Stevens, F. J. *Protein Eng.* **1992**, *5*, 213–214.
- (11) Landolt-Marticorena, C.; Williams, K. A.; Deber, C. M.; Reithmeier, R. A. F. *J. Mol. Biol.* **1993**, *229*, 602–608.
- (12) Killian, J. A.; Salemink, I.; De Planque, M. R.; Lindblom, G.; Koeppe, R. E., II; Greathouse, D. V. *Biochemistry* **1996**, *35*, 1037–1045.
- (13) Bradley, K. A.; Mogridge, J.; Mourez, M.; Collier, R. J.; Young, J. A. T. *Nature* **2001**, *414*, 225–229.

within their respective monolayers by four tryptophans in each subunit.<sup>14</sup>

Gramicidin A (gA) has the sequence formyl-VGALA<sup>1</sup>VVW<sup>9</sup>LW<sup>11</sup>LW<sup>13</sup>LW<sup>15</sup>-ethanolamide, in which D-amino acids are italicized. For the gramicidin channel in lipid bilayers of DMPC, there have been several reports of spectral analysis of ring-perdeuterated Trp side chains.<sup>15–18</sup> The full potential of <sup>2</sup>H spectra of labeled Trps in any membrane-spanning structure, nevertheless, has yet to be realized because of lingering uncertainties about some of the spectral assignments<sup>16,17</sup> and the ring geometry.<sup>5,6,19,20</sup> Some past analyses from our lab and others have been plagued by a lack of attention to the planarity of the indole ring.<sup>5</sup> In early energy minimizations,<sup>21</sup> we noted tendencies for the program Discover to distort indole rings away from planarity (M. J. Taylor and R. E. Koeppe, unpublished results). Apparent distortions from a planar indole geometry have emerged also during structure refinement.<sup>22</sup> Such distortions would influence the interpretation of <sup>2</sup>H NMR spectra.

As a recent article stated, “it is important to realize that the precision at which the indole geometry can be derived from the literature or any database is rather limited”.<sup>6</sup> In the present study, we use a partial labeling strategy to label selectively positions C2 and C5 of the indole ring, thus yielding unambiguous spectral assignments. Then, using methods that are independent of assumptions concerning a particular backbone-folding, we establish a precise side-chain ring geometry using first an experimental and then a theoretical method. The results of these two approaches are in agreement, and we conclude that the indole ring is planar yet asymmetric, particularly in its five-membered ring. The geometric considerations explain previously noted systematic discrepancies in predicted indole C–<sup>2</sup>H bond orientation angles<sup>16</sup> and impose an obligatory revision of an early spectral assignment scheme for *d*<sub>5</sub>-Trp-9 in gA.<sup>16</sup> Finally, we use the revised indole ring geometry to define the backbone-independent orientations for tryptophans 9, 11, 13, and 15 in the gA channel in DMPC bilayers.

## Materials and Methods

**Selective Labeling of the Indole Ring.** The methods for partial deuterium exchange on the indole ring were adapted from Bak et al.<sup>23,24</sup> Fmoc-L-Trp (0.1 mmol) from Advanced ChemTech (Louisville, KY) was dissolved in 400  $\mu$ L of trifluoroacetic acid–<sup>2</sup>H (CF<sub>3</sub>COO–<sup>2</sup>H) from Cambridge Isotope Laboratories (Andover, MA) and incubated for 45 min to 6 h at 4 °C or room temperature (22 °C) in darkness. Exposure to light, and/or the (extended) use of elevated temperatures, increased the likelihood and extent of damage to the Trp side chain. The reaction

**Table 1.** Observed Position-Dependent Deuterium Exchange on the Indole Ring of Fmoc-L-Trp<sup>a</sup>

temp (°C)	time (min)	H2	H4	H5	H6	H7
4	45	37	0	7	4	0
4	120	67	0	29	15	0
4	180	70	0	21	<10	0
4	360	72	0	23	10	0
22	45	77	10	48	19	7
22	120	71	7	49	15	4
22	240	84	~20	78	40	~20

<sup>a</sup> Percentage of exchange (loss of <sup>1</sup>H NMR signal) after exposure to CF<sub>3</sub>COO–<sup>2</sup>H at either 4 °C or room temperature (~22 °C), for the indicated periods of time. The values are reproducible to  $\pm 10\%$  absolute exchange for triplicate samples.

was quenched by addition of 1 mL cold D<sub>2</sub>O, and the exchanged Fmoc-L-Trp was isolated by centrifugation (13 000 rpm at 4 °C). The product was washed once with D<sub>2</sub>O and then twice with H<sub>2</sub>O at 22 °C and dried under vacuum (10<sup>–3</sup> mmHg). The resulting selective exchange of indole ring hydrogens was monitored by following the reductions in the respective aromatic <sup>1</sup>H peak intensities in <sup>1</sup>H NMR spectroscopy. No damage to Fmoc-L-Trp was observed from the <sup>1</sup>H NMR spectra. Based on the observed extent of isotope exchange as functions of ring position and time of incubation (Table 1), an exchange reaction time of 180 min at 4 °C was selected to prepare Fmoc-L-Trp for peptide synthesis. The resulting amino acid derivative was used without further purification but was predissolved in *N*-methylpyrrolidinone prior to automated peptide synthesis. As also suggested by the lack of <sup>1</sup>H/<sup>2</sup>H exchange at the C $\alpha$  position, analysis using a chirobiotic-T HPLC column (Advanced Separation Technologies, Inc., Whippany, NJ) confirmed that no racemization occurred during the exchange reaction.

For fully labeled ring *d*<sub>5</sub>-L-Trp, the labeled amino acid was purchased from Cambridge Isotope Laboratories (Andover, MA) and was converted to the Fmoc derivative as previously described.<sup>25</sup>

**Peptide Synthesis.** Gramicidins that incorporate a single partially or fully labeled tryptophan indole ring were synthesized on a 0.1 mmol scale as previously described,<sup>25</sup> using a 5-fold molar excess of the labeled or unlabeled amino acids.

**Analysis.** Deuterium NMR spectroscopy was performed using oriented samples of labeled gA in hydrated DMPC (1:10 to 1:40 molar ratio of peptide/lipid), as described previously.<sup>4,26</sup> Typically, a dried film consisting of 4  $\mu$ mol of labeled gA and 80  $\mu$ mol of DMPC (Avanti Polar Lipids, Alabaster, AL) was resuspended in either 0.8 mL of chloroform or 1 mL of 95% methanol, 5% water. The sample was applied evenly to 42–46 glass plates of size 4.8  $\times$  23.0 mm<sup>2</sup> (thickness 00; 0.06–0.08 mm; Marienfeld Glassware, Lauda-Königshofen, Germany). After extensive drying under vacuum, the plates were hydrated with 40–50  $\mu$ L of <sup>2</sup>H-depleted H<sub>2</sub>O and stacked. Sample alignment was facilitated by applying some pressure to the stacked plates.<sup>4</sup> The stack was inserted into a glass cuvette, which was sealed with an end-plate and quick-drying epoxy, and incubated a minimum of 72 h at 40 °C.

NMR measurements were performed at 40 °C to ensure that the lipids were in the liquid-crystalline phase. Lipid alignment within the samples was measured by oriented solid-state <sup>31</sup>P NMR with proton decoupling, using a custom probe from Doty Scientific (Columbia, SC) and a Bruker AMX2 300 spectrometer, modified for wide-line operation. Oriented deuterium NMR experiments were performed at 46.1 MHz, using a quadrupolar echo pulse sequence with full phase cycling,<sup>27</sup> with a 3  $\mu$ s pulse time, a 60  $\mu$ s echo delay, and a sweep width of 2.5 MHz. Experiments in which the interpulse time was varied

(14) O’Connell, A. M.; Koeppe, R. E., II; Andersen, O. S. *Science* **1990**, *250*, 1256–1259.

(15) Hu, W.; Lee, K. C.; Cross, T. A. *Biochemistry* **1993**, *32*, 7035–7047.

(16) Koeppe, R. E., II; Killian, J. A.; Greathouse, D. V. *Biophys. J.* **1994**, *66*, 14–24.

(17) Hu, W.; Lazo, N. D.; Cross, T. A. *Biochemistry* **1995**, *34*, 14138–14146.

(18) Cotten, M.; Tian, C.; Busath, D. D.; Shirts, R. B.; Cross, T. A. *Biochemistry* **1999**, *38*, 9185–9197.

(19) Koeppe, R. E., II; Killian, J. A.; Vogt, T. C. B.; De Kruijff, B.; Taylor, M. J.; Mattice, G. L.; Greathouse, D. V. *Biochemistry* **1995**, *34*, 4, 9299–9306.

(20) Separovic, F.; Ashida, J.; Woolf, T.; Smith, R.; Terao, T. *Chem. Phys. Lett.* **1999**, *303*, 493–498.

(21) Killian, J. A.; Taylor, M. J.; Koeppe, R. E., II. *Biochemistry* **1992**, *31*, 11283–11290.

(22) Ketchum, R. R.; Roux, B.; Cross, T. A. *Structure* **1997**, *5*, 1655–1669.

(23) Bak, B.; Dambmann, C.; Nicolaisen, F. *Acta Chem. Scand.* **1967**, *21*, 1674–1675.

(24) Bak, B.; Led, J. J.; Pedersen, E. J. *Acta Chem. Scand.* **1969**, *23*, 3051–3054.

(25) Greathouse, D. V.; Koeppe, R. E., II; Providence, L. L.; Shobana, S.; Andersen, O. S. *Methods Enzymol.* **1999**, *294*, 525–550.

(26) Koeppe, R. E., II; Vogt, T. C. B.; Greathouse, D. V.; Killian, J. A.; De Kruijff, B. *Biochemistry* **1996**, *35*, 3641–3648.

(27) Davis, J. H.; Jeffrey, K. R.; Bloom, M.; Valio, M. I.; Higgs, T. P. *Chem. Phys. Lett.* **1976**, *42*, 390–394.

from 30 to 900 ms showed no significant changes in the spectra. The aligned samples were measured in two different orientations: with the normal to the lipid bilayers aligned either parallel to the applied magnetic field ( $\beta = 0^\circ$ ) or perpendicular to it ( $\beta = 90^\circ$ ). After application of a 500 Hz line-broadening to the spectra, the magnitude of the quadrupolar splitting ( $\Delta\nu_q$ ) of each doublet was determined as the distance between the peak maxima. Experiments in which the peptide/lipid ratio was varied between 1:10 and 1:40 gave identical quadrupolar splittings.

Once the spectral assignments were confirmed by partial specific labeling of the indole rings (see results), consideration turned to the indole ring geometry, orientation, and dynamics to fit the sets of observed quadrupolar splittings to the equation:<sup>21</sup>

$$\Delta\nu_q = ({}^3/2)(e^2qQ/h)({}^{1/2}[3 \cos^2 \theta - 1])({}^{1/2}[3 \cos^2 \beta - 1])(1)$$

in which  $e^2qQ/h$  is the C–<sup>2</sup>H quadrupolar coupling constant (QCC;  $\sim 180$  kHz for aromatic deuterons<sup>28</sup>),  $\theta$  is the angle between a C–<sup>2</sup>H bond and the axis of rapid global molecular reorientation, which is coincident with the membrane normal, and  $\beta$  is the angle between the membrane normal and the magnetic field,  $\mathbf{H}_0$ . This equation is based upon the premise that the principal component of the electric field gradient tensor,  $\mathbf{V}_{zz}$ , is aligned very close to the C–<sup>2</sup>H bond,<sup>29</sup> and that the asymmetry parameter  $\eta = (|\mathbf{V}_{yy}| - |\mathbf{V}_{xx}|)/\mathbf{V}_{zz}$  is small.<sup>17,28,30</sup> Small nonzero values of  $\eta$  are expected to have minor effects and will not be considered here. As in previous analyses,<sup>5,15–18</sup> the basic strategy was to adjust the orientation of an indole ring of fixed geometry with respect to the membrane normal in such a way as to maximize the agreement between the  $\theta$  values for deuterons around the ring and the  $\Delta\nu_q$  values observed in the NMR spectra.

Indole ring motions will cause the “effective” QCC to be reduced from the static value of 180 kHz. This reduction can be estimated based on the multiplier  $S_{zz}$ , the principal order parameter about the long axis of molecular reorientation (the helix axis) of the gramicidin channel.<sup>31</sup>  $S_{zz}$  is similar to the motional-narrowing factor defined by Prosser and Davis.<sup>30</sup> Approximations based upon a principal order parameter are valid when the principal motions are fast diffusion about the long symmetry axis, (small) reorientations of the long axis with respect to the external magnetic field, and (small) reorientations of individual indole rings with respect to the long axis (see Discussion). The measured  $S_{zz}$  of 0.93 for backbone atoms<sup>21,30–32</sup> represents an upper limit for the side-chain indole rings.

To establish a method of data analysis that would be independent of a particular backbone conformation or backbone assumptions, we chose first to orient a hypothetical “free” indole ring with respect to the membrane normal and  $\mathbf{H}_0$ , using the angles  $\rho_1$  and  $\rho_2$  defined in Figure 1. (In later analyses, these “free indole” results can be related to particular backbone models; see below.) To implement the method, the ring initially is aligned so that the bridge between the five- and six-membered rings is parallel to the membrane normal and an origin is chosen at the midpoint of the bridge. Two rotation angles then serve to tip the ring through all possible orientations: first,  $\rho_1$  about the normal to the ring through the origin and, second,  $\rho_2$  about an axis through the origin that is normal to both the bridge and the axis of  $\rho_1$  rotation (Figure 1).

**Indole Ring Geometry.** We derived starting planar indole coordinates from the library of aromatic rings in InsightII (version Insight 2000 from Accelrys Corp., San Diego, CA); the model was characterized by symmetric five- and six-membered rings with 1.4 Å bond

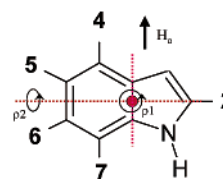


**Figure 1.** Idealized free indole ring showing reference angles  $\rho_1$  and  $\rho_2$  for rotation. For fitting the ring orientation to a set of known, assigned <sup>2</sup>H quadrupolar splittings, the ring is initially aligned with the bridge (C8–C9 bond) parallel to the magnetic field,  $\mathbf{H}_0$ . The ring is then rotated incrementally about two axes normal to the bridge, first through angle  $\rho_1$  and then through angle  $\rho_2$ , to obtain the best fit to the observed quadrupolar splittings for deuterons attached to C2, C4, C5, and C6. (Usually, the quadrupolar splittings for C4- and C7-deuterons are essentially indistinguishable (Figures 2 and 3); see text for details.)

lengths for C–N as well as C–C bonds. Following preliminary calculations using the symmetric indole, we continued the analysis in two ways: first, by manually changing the direction of the C2–<sup>2</sup>H bond in the symmetric indole ring and, second, by ab initio calculations of the bona fide indole ring geometry.

**ab Initio Calculations.** The initial geometry of Trp’s indole side chain was generated by the semiempirical PM3 method<sup>33</sup> and was further optimized with the hybrid B3-LYP density functional, using three successively larger basis sets: 3-21G, 6-31G\*, and 6-311G\*\*. To simulate geometry of a ring attached to a side-chain  $\beta$ -carbon, all calculations were performed on 3-methyl-indole by implementing the PQS suite of quantum chemistry programs.<sup>34</sup> As anticipated for such a rigid molecule, the three geometries agreed closely. The indole side-chain orientations presented herein utilize the geometry generated from the B3-LYP/6-311G\*\* calculation. B3-LYP calculations with larger basis sets such as the ones used in this paper give very accurate equilibrium geometries for organic molecules.<sup>35</sup> Comparison with experiment is limited mainly by experimental uncertainties but is well below 0.01 Å and a few tenths of a degree for rigid, experimentally well-characterized molecules, such as porphyrin.<sup>36</sup>

The substitution of deuterium for hydrogen has no effect on equilibrium geometries as calculated here. In the vibrationally averaged structure, C–<sup>2</sup>H bonds are slightly ( $\sim 0.01$  Å) shorter than C–H bonds, because of the asymmetry of the stretching potential function. The effect on the C–H bond angles, where the potential is much more symmetric, is expected to be virtually nil; indeed the differences between average or equilibrium bond angles are less than a few tenths of a degree.

**Backbone Connections.** Following the virtual “free indole” analysis (above), using the corrected ring geometry, we correlated the determined orientations for tryptophans 9, 11, 13, and 15 to several experimental models for the backbone of gA, namely structures IMAG<sup>22</sup> and IJNO<sup>37</sup> in the Protein Data Bank, and with a locally refined version<sup>21</sup> of the early Arseniev model.<sup>38</sup> The purpose of this analysis was to examine the ranges of Trp ( $\chi_1$ ,  $\chi_2$ ) angles for these backbone models that are consistent with the free indole analysis. Figures 7 and 8 were generated using PyMol (<http://www.pymol.org>).

## Results

**Indole Ring Spectral Assignments.** Questions about the spectral assignments for deuterated indole rings in gramicidin A channels were resolved by partial specific labeling. Figure 2 shows the <sup>2</sup>H NMR spectra for oriented gA channels having a

(28) Gall, C. M.; DiVerdi, J. A.; Opella, S. J. *J. Am. Chem. Soc.* **1981**, *103*, 5039–5043.  
 (29) Seelig, J. Q. *Rev. Biophys.* **1977**, *10*, 353–418.  
 (30) Prosser, R. S.; Davis, J. H.; Dahlquist, F. W.; Lindorfer, M. A. *Biochemistry* **1991**, *30*, 4687–4696.  
 (31) Separovic, F.; Pax, R.; Cornell, B. *Mol. Phys.* **1993**, *78*, 357–369.  
 (32) Hing, A. W.; Adams, S. P.; Silbert, D. F.; Norberg, R. E. *Biochemistry* **1990**, *29*, 4144–4156.

(33) Stewart, J. J. P. *J. Comput. Chem.* **1989**, *10*, 209–220.  
 (34) PQS, version 2.4; Parallel Quantum Solutions: 2013 Green Acres Road, Fayetteville, Arkansas, 72703.  
 (35) Baker, J.; Pulay, P. *J. Chem. Phys.* **2002**, *117*, 1441–1449.  
 (36) Kozłowski, P. M.; Zgieraki, M. Z.; Pulay, P. *Chem. Phys. Lett.* **1995**, *247*, 379–385.  
 (37) Townsley, L. E.; Tucker, W. A.; Sham, S.; Hinton, J. F. *Biochemistry* **2001**, *40*, 11676–11686.  
 (38) Arseniev, A. S.; Lomize, A. L.; Barsukov, I. L.; Bystrov, V. F. *Biol. Membr.* **1986**, *3*, 1077–1104.



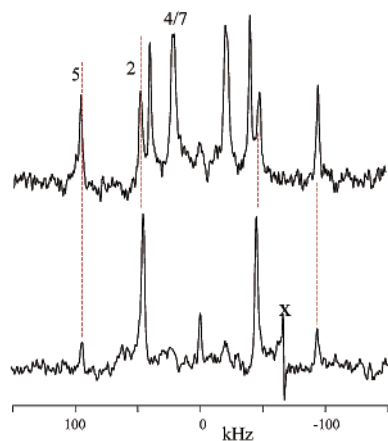


**Figure 2.**  $^2\text{H}$  NMR spectra for ring-labeled Trp-11 in oriented samples of gramicidin A in hydrated DMPC. (Upper) Ring uniformly labeled at C2, C4, C5, C6, and C7. (Lower) Ring selectively labeled at C2 and C5. (The spike marked “X” is an instrumental artifact.) Temperature, 40 °C. Sample orientation,  $\beta = 0^\circ$ .

fully deuterated or a specifically (C2/C5) deuterated indole ring at Trp-11. The signals from the C2- and C5-deuterons are clearly distinguishable because of the differing extents of deuterium incorporation:  $\sim 70\%$  at C2 and  $\sim 20\%$  at C5 (Table 1). The C5- $^2\text{H}$  resonance is in obvious agreement with earlier assignment schemes, from molecular modeling,<sup>16,17</sup> which assigned this resonance the largest quadrupolar splitting ( $|\Delta\nu_q|$  of 191 kHz for the  $\beta = 0^\circ$  sample orientation, with the membrane normal parallel to  $\mathbf{H}_0$ ) in the spectrum for fully ring-deuterated Trp-11. The signals from the C2- and C6-deuterons of  $d_5$ -Trp-11 actually are quite close to each other (upper spectrum of Figure 2) and were misassigned (interchanged) in earlier modeling schemes.<sup>16,17</sup> The lower spectrum of Figure 2 shows that the C2- $^2\text{H}$  resonance has the second largest quadrupolar splitting, with  $|\Delta\nu_q| = 96$  kHz. (We attribute the earlier assignment error (from our lab) to an incorrect indole ring geometry; see below.) With the C2 and C5 positions assigned, and the combined resonances from the geometrically similar C4/C7-deuterons showing obvious twinning at 39/41 kHz, as noted previously,<sup>16,17</sup> the remaining resonance ( $|\Delta\nu_q| = 79$  kHz) can be assigned to the C6 position in Trp-11.

A similar partial ring labeling experiment was used to assign the  $^2\text{H}$  NMR spectrum for Trp-9 in gA (Figure 3). Because the spectra for this ring show no obvious twinning of the C4- $^2\text{H}$ /C7- $^2\text{H}$  resonances, the assignments for Trp-9 have been particularly problematic; in fact, it was shown that four different assignment schemes are consistent with the  $^2\text{H}$  NMR spectrum for Trp-9 in gA.<sup>17</sup> For partially deuterated Trp-9, one sees only the C2- $^2\text{H}$  resonance for the  $\beta = 0^\circ$  sample orientation in DMPC (middle spectrum in Figure 3), because the C5- $^2\text{H}$  enrichment is only  $\sim 20\%$  and its quadrupolar splitting is large. Nevertheless, the C5- $^2\text{H}$  signal intensity increases when  $|\Delta\nu_q|$  is reduced by  $1/2$ , as the sample is turned by  $90^\circ$  with respect to  $\mathbf{H}_0$  (bottom spectrum in Figure 3). With  $|\Delta\nu_q|$  values of 43 kHz for C2- $^2\text{H}$  and 151 kHz for C5- $^2\text{H}$  evident in Figure 3, the “most probable” Trp-9 assignment scheme predicted by Hu et al.<sup>17</sup> is confirmed (see Table 2).

Table 2 summarizes the  $^2\text{H}$  spectral assignments for all of the Trp indole rings in oriented, hydrated gA channels in lipid bilayers of DMPC. (The signs of the  $\Delta\nu_q$  values were determined by molecular modeling; see below.)

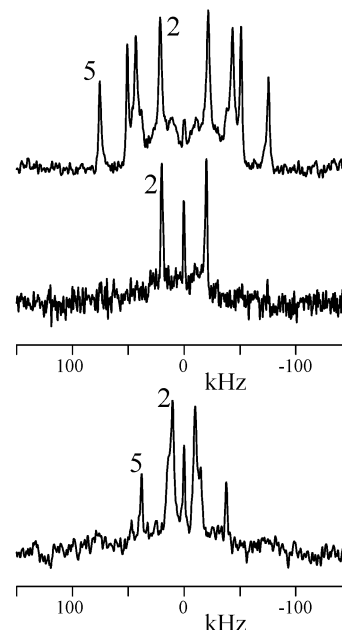


**Figure 3.**  $^2\text{H}$  NMR spectra for ring-labeled Trp-9 in oriented samples of gramicidin A in hydrated DMPC. (Top) Ring uniformly labeled at C2, C4, C5, C6, and C7; sample orientation  $\beta = 0^\circ$ . (Middle) Ring selectively labeled at only C2 and C5; sample orientation  $\beta = 0^\circ$ . (Bottom) Ring selectively labeled at C2 and C5; sample orientation  $\beta = 90^\circ$ . Temperature, 40 °C.

**Table 2.**  $^2\text{H}$  Quadrupolar Splittings ( $\Delta\nu_q$ , in kHz) and Assignments for Trp Rings in Oriented Gramicidin A Channels in DMPC<sup>a</sup>

ring position/sequence position	Trp-9	Trp-11	Trp-13	Trp-15
2	43	96	106	125
4/7	86	39/41	30/32	0/2
5	151	188	205	205
6	-102	-79	-81	-61

<sup>a</sup> The  $^2\text{H}$  NMR resonances of ring positions 2 and 5 were assigned from the spectra for partially labeled rings (Figures 2 and 3), of positions 4/7 by the “twinning” of closely related peaks (e.g., Figure 2) and of position 6 by molecular modeling. The magnitudes of  $\Delta\nu_q$  values were measured from peak separations in spectra such as those in Figures 2 and 3, to an estimated accuracy of  $\pm 1$  kHz; therefore, we do not profess to distinguish the individual assignments for positions 4 and 7. The signs ( $\pm$ ) for the  $\Delta\nu_q$  values were allowed to vary during the ring orientation fitting procedure and emerged unambiguously during the calculation of spectra from the molecular models. The assignment patterns are consistent with those of Hu et al.,<sup>17</sup> with a small change for Trp-11.

**C2- $^2\text{H}$  Bond Orientation.** In addition to the spectral assignments, accurately known indole C- $^2\text{H}$  bond directions are necessary for effective modeling of the Trp side-chain ring orientations in membrane-spanning peptides. As a starting model, we chose a flat indole ring from the InsightII library. In hindsight, the model is too symmetric, in that the C-N and C-C bond lengths are identical (1.4 Å). Nevertheless, this initial model had the advantage of being rigorously flat,<sup>39–41</sup> and it allowed us to refine the C2- $^2\text{H}$  bond (i.e., the  $\mathbf{V}_{zz}$  component of the field gradient tensor) orientation against experimental data in a systematic way. In initial attempts to fit the observed, assigned quadrupolar splittings using the known spectral assignments, we were unable to obtain satisfactory agreement for any of the tryptophans in gA using the symmetric ring template. (The calculated rmsd remained  $> 6$  kHz for each Trp, although

(39) Harada, Y.; Iitaka, Y. *Acta Crystallogr.* **1977**, *B33*, 244–247.

(40) Souhassou, M.; Lecomte, C.; Blessing, R. H.; Aubry, A. *Acta Crystallogr.* **1991**, *B47*, 253–266.

(41) Caminati, W.; Di Bernardo, S. *J. Mol. Struct.* **1990**, *240*, 253–262.

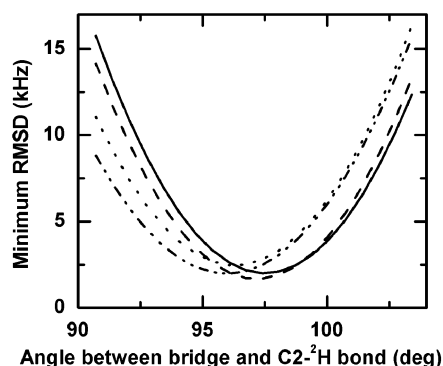


**Figure 4.** Dependence of the lowest achievable rmsd on the angle between the C2–<sup>2</sup>H bond vector and the indole ring bridge (C8–C9 bond). For each particular indole ring geometry, the ring was rotated through all possible orientations (using  $\rho_1$  and  $\rho_2$ ; see Figure 1),  $S_{zz}$  for the ring was varied, and the minimum rmsd's corresponding to the global best fits to the <sup>2</sup>H NMR spectra for Trp-9 (—), Trp-11 (---) Trp-13 (· · · · ·), and Trp-15 (— · — · —) in gramicidin A were computed. See text for details.

the measured quadrupolar splittings are known to within  $\pm 1$  kHz.) We noticed a systematic discrepancy at C2 along with an internal consistency among the quadrupolar splittings for “phenyl” ring positions, as we could fit simultaneously the data for the C4-, C5-, and C6-deuterons on the six-membered ring of each Trp very well but not for the C2-deuteron.

Two possibilities, which are not mutually exclusive, could explain the discrepancy: the C2–<sup>2</sup>H bond is not perpendicular to the ring bridge and/or the quadrupolar spin interaction tensor in question could deviate significantly from the C2–<sup>2</sup>H bond direction.<sup>16,28</sup> Our analysis indicated that the bond direction itself is responsible for most of the initial discrepancy (see below) as well as for an earlier incorrect assignment of the <sup>2</sup>H NMR spectrum for *d*<sub>5</sub>-Trp-9 in gA.<sup>16</sup>

Maintaining an entirely flat indole ring system, we varied the orientation of the C2–<sup>2</sup>H bond with respect to the ring bridge (keeping all other coordinates fixed). The C2-deuteron was moved manually so that the angle between the ring bridge and the C2–<sup>2</sup>H bond varied in increments of 0.05°. Each revised indole ring was rotated through all possible ( $\rho_1$ ,  $\rho_2$ ) angles (Figure 1). At each orientation, the ring  $S_{zz}$  was allowed to vary in increments of 0.02, and the predicted quadrupolar splittings were compared against the data set for each Trp, 9, 11, 13, and 15, in gA. For each particular C2–<sup>2</sup>H geometry, the global minimum rmsd for fitting each of the four data sets was computed, producing the results shown in Figure 4. Remarkably, each Trp data set gives a best fit with a minimum rmsd in the range 1.5–2.5 kHz at a closely similar angle between the bridge and the C2–<sup>2</sup>H bond. The minima in Figure 4 occur at 96.2°  $\pm$  1.0° for the four data sets.

The results in Figure 4 could, in principle, suggest a significant off-bond component for the C2–<sup>2</sup>H spin interaction tensor. To test this possibility, we performed ab initio calculations to predict the indole ring geometry. Results from the different basis sets (see Materials and Methods) were quite similar to each other; the final calculation using the 6-311G\*\* basis set gave the coordinates listed in Table 3. The indole described by the coordinates in Table 3 remains flat but has a slight asymmetry in the six-membered ring and a more pronounced asymmetry in the five-membered ring, mainly due to the fact that C–N bond distances differ from C–C bond distances. The angles between the C2–H bond and the C8–

**Table 3.** Final Indole Ring Coordinates (Å) from ab Initio Calculation on 3-Methyl Indole<sup>a</sup>

atom	x	y
N1	1.317	−1.115
NH1	1.636	−2.068
C2	2.134	0.003
H2	3.208	−0.105
C3	1.375	1.142
C4	−1.231	1.387
H4	−1.262	2.471
C5	−2.405	0.651
H5	−3.361	1.163
C6	−2.381	−0.757
H6	−3.316	−1.305
C7	−1.182	−1.455
H7	−1.165	−2.540
C8	0	−0.711
C9	0	0.711

<sup>a</sup> These coordinates were used to generate the contour plots in Figure 5. The ab initio calculations predict that the ring is planar, with a z-coordinate of zero for each atom. As Supporting Information, we provide also coordinates for *N*-acetyl-tryptophan-methylamide.

C9 bridge were calculated to be 95.83° when using the 6-31G\* basis set and 95.75° with the 6-311G\*\* basis set. We conclude that the indole C2–<sup>2</sup>H bond direction is quite similar to the experimentally determined direction of the  $\mathbf{V}_{zz}$  tensor component. Indeed, ab initio calculations indicate that the principal  $\mathbf{V}_{zz}$  tensor component at each ring position differs from the respective C–<sup>2</sup>H bond direction by only 0.01°–0.11°. (The asymmetry parameter  $\eta = (|V_{yy}| - |V_{xx}|)/V_{zz}$  could have a small influence,<sup>28</sup> but we do not consider nonzero values of  $\eta$  here.) The major result from the ab initio calculations concerns the offset of the indole C2–<sup>2</sup>H bond direction from the normal to the ring bridge. Also in the refined indole model, the C4–<sup>2</sup>H and C7–<sup>2</sup>H bonds are no longer strictly parallel; while this result may suggest an experimental basis for distinguishing the quadrupolar splittings from C4- and C7-deuterons, the difference still will be comparable to the experimental errors of measurement, and we will not deal further with the issue here.

**Trp Indole Orientations and Dynamics in the Gramicidin A Channel.** With the refined indole ring geometry available (Table 3), we sought an analysis that would compare the orientations of the Trp-9, -11, -13 and -15 rings with respect to the bilayer membrane normal, independent of any assumptions about the backbone-folding (see Materials and Methods). To this end, we refined the  $\rho_1$  and  $\rho_2$  angles (Figure 1) and  $S_{zz}$  for each ring against the data sets in Table 2. This procedure will yield eight identical solutions, one of which will appear within the octant where  $\rho_1$  ranges from 0° to 90° and  $\rho_2$  ranges from 0° to 180°. Note that, within the context of the bilayer environment, with the coordinate system defined with respect to the bilayer normal, all eight solutions reflect in essence the same ring orientation. The results are shown by the contour plots in Figure 5, and the best-fit values for  $\rho_1$ ,  $\rho_2$ , and  $S_{zz}$  for each ring are listed in Table 4.

The ( $\rho_1$ ,  $\rho_2$ ) contour plots in Figure 5 were drawn for the particular best-fit value of  $S_{zz}$  for each Trp ring. To estimate the uncertainties in the  $\rho_1$ ,  $\rho_2$ , and  $S_{zz}$  parameters, we examined the variation of the best-fit  $\rho_1$  and  $\rho_2$  angles and the corresponding minimum rmsd as functions of  $S_{zz}$  for each of the Trp indole rings. The results for Trp-9 are shown graphically in Figure 6. Solutions with an rmsd < 3.0 kHz are found within a range of  $\pm 0.04$  relative to the “optimal”  $S_{zz}$ , as is listed also in Table 4 (with more specific data for Trp-11 in the footnote).

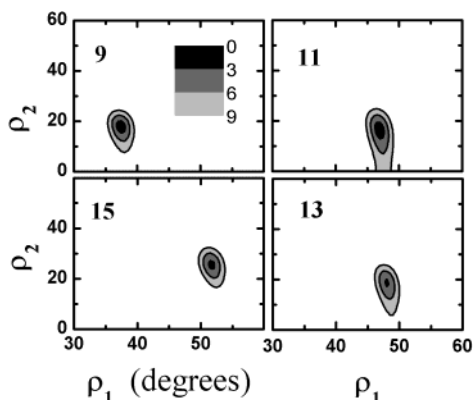


**Figure 5.** Contour plots for free indole rotation. Each indole ring in gA gave a unique solution within the octant  $0^\circ$ – $90^\circ$  in  $\rho_1$  and  $0^\circ$ – $180^\circ$  in  $\rho_2$ . An expanded region of rotational space from  $30^\circ$  to  $60^\circ$  in  $\rho_1$  and  $0^\circ$  to  $60^\circ$  in  $\rho_2$  is shown. The  $S_{zz}$  values used to generate the plots are listed in Table 4. The scale for the contours indicates rmsd in units of kHz.

**Table 4.** Orientations of Trp-9, -11, -13, and -15 Indole Rings with Respect to the Bilayer Membrane Normal<sup>a</sup>

Trp	$\rho_1$	$\rho_2$	$S_{zz}$	minimum rmsd (kHz)
9	$37.5^\circ$	$18.0^\circ$	$0.80 \pm 0.03$	0.38
11	$47.0^\circ$	$16.0^\circ$	$0.80 \pm 0.03$	0.58
13	$48.0^\circ$	$18.5^\circ$	$0.88 \pm 0.04$	2.59
15	$51.5^\circ$	$25.5^\circ$	$0.86 \pm 0.04$	2.35

<sup>a</sup> The angles  $\rho_1$  and  $\rho_2$  (Figure 1) were searched in  $0.5^\circ$  increments, while  $S_{zz}$  values were searched in increments of 0.006. The rmsd values correspond to the global minima (comparing observed and calculated quadrupolar splittings). The listed tolerance for  $S_{zz}$  represents the range of  $S_{zz}$  yielding an rmsd less than 3.0 kHz. When  $S_{zz}$  (for Trp-11) was changed by  $\pm 0.03$  from its optimum,  $\rho_1$  varied by  $\pm 0.5^\circ$ ,  $\rho_2$  varied by  $\pm 4.0^\circ$ , and the rmsd increased from 0.58 to 1.9 kHz.

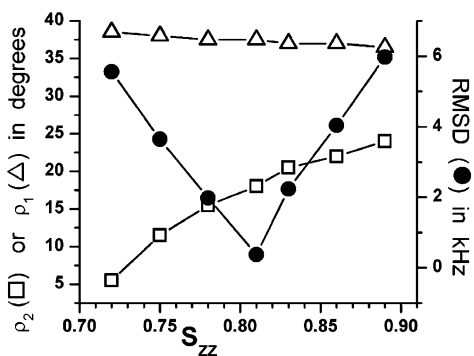


**Figure 6.** Graph to show the variation of the best-fit  $\rho_1$  and  $\rho_2$  and the value of the corresponding rmsd minimum as functions of  $S_{zz}$  for the Trp-9 indole ring.

Results for the other tryptophans were similar. Figure 6 shows that  $\rho_1$  is quite insensitive to changes in  $S_{zz}$  and that  $\rho_2$  is 5–10 times more sensitive. For all Trps, on average,  $\rho_1$  changes by only  $1.0^\circ$ , and  $\rho_2$ , by  $5^\circ$ – $10^\circ$  for a change of 0.06 in  $S_{zz}$ .

Despite the obvious spectral differences (Table 2 and ref 17), the refined average orientations of the Trp indole rings in membrane-spanning gramicidin channels are quite similar to each other. The largest deviations from a common orientation with respect to the membrane normal (Table 4) are that Trp-9 differs from the others by  $10^\circ$ – $15^\circ$  in  $\rho_1$  and Trp-15 differs from the others by  $7^\circ$ – $10^\circ$  in  $\rho_2$ . Indeed, the largest difference between any pair of rings is found for the Trp-9/Trp-15 “pair.” Figure 7 shows a top view of the gA indole rings, looking down the membrane normal.

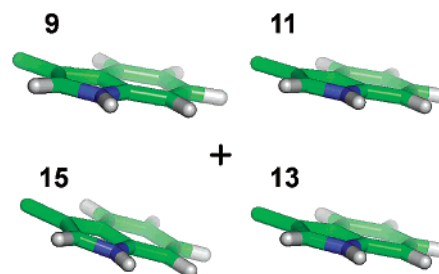


**Figure 7.** End view showing the average orientation, with respect to a membrane surface, for each indole ring, 9, 11, 13, and 15 of the gramicidin A channel, looking down a lipid bilayer membrane normal (denoted by “+”).

The indole ring orientations represented in Figures 5 and 7 are the time-averaged ring orientations that best fit the  $^2\text{H}$  NMR spectral data. In the absence of ring motion, the aromatic ring-attached deuterons exhibit a static QCC of 180 kHz.<sup>28</sup> The principal order parameter of 0.93 for backbone atoms<sup>31</sup> will reduce this value. Local ring motions (anisotropic “wobbling”) will reduce the “effective” QCC still further, to a greater or lesser extent for each deuteron on the indole ring. Although the extent of QCC reduction will vary somewhat with the average ring orientation, ring position, and type of motion<sup>17</sup> (see Discussion), the limited size of the data sets for the Trps in gA (Table 2) allowed us only an approximate approach, that is, an estimation of an overall  $S_{zz}$  for each ring. The “best-fit” values of  $S_{zz}$  correspond to “effective” QCC values of 144 kHz for Trp-9 and Trp-11 and 155–158 kHz for Trp-13 and Trp-15. Although approximate, the approach leads to two observations: (a) the two “inner” rings of Trp-9 and Trp-11 (that are marginally farther from the membrane/water interface) exhibit somewhat greater motional freedom than do the two “outer” rings of Trp-13 and Trp-15 (that are closer to the interface) and (b) the approximation gives an apparently better fit (lower rmsd in Table 4) for the inner Trps 9 and 11 than for the outer Trps 13 and 15. The reason for the latter observation is unclear but might reflect a poorer approximation of the actual motion of these more highly constrained rings when using the  $S_{zz}$  parameter. Because side chains are attached to the backbone via somewhat flexible linkers (which may allow additional motion), one anticipates that 0.93 should be an upper limit for  $S_{zz}$  for side-chain deuterons. Indeed the fitted  $S_{zz}$  values are 0.80 and 0.86–0.88, respectively, for the “inner” and “outer” pairs of Trp rings (i.e., only slightly less than the values for backbone atoms).

## Discussion

We report the use of site-specific partial  $^2\text{H}$  labeling of Trp indole rings for spectral assignment which, together with ab initio calculations, allows us to deduce an indole ring geometry that is in remarkable agreement with both experimental observations and theoretical predictions. This refined indole ring geometry has broad potential for the future molecular modeling of Trp residues in soluble as well as membrane proteins. To illustrate the method, we use the revised geometric considerations to resolve several questions and problems concerning the  $^2\text{H}$  NMR spectra of Trp indole rings in membrane-spanning gramicidin channels. We describe also an approach that permits analysis of (hypothetical) “free ring” orientations for tryptophans



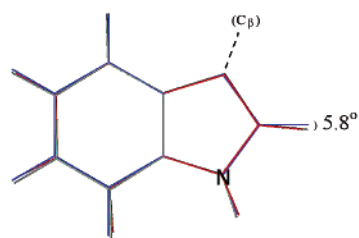


**Figure 8.** Overlay of three models for the planar indole ring: (a) averaged coordinates from two X-ray crystal structures of acetyl-tryptophan-methylamide<sup>39,40</sup> (red), (b) results from ab initio calculation on 3-methyl indole (Table 3; gray), (c) a symmetric model with equivalent 1.4 Å bonds (see Materials and Methods; blue). For non-hydrogen atoms, the rms deviations in the *x* and *y* in-plane coordinates, compared to the averaged X-ray model, are 0.014 Å for the ab initio model and 0.026 Å for the symmetric model. (The rms deviation is 0.028 Å between the two X-ray models.) The attachment of indole to C<sub>β</sub> of Trp is shown schematically. The figure also illustrates the salient result from the ab initio model and X-ray models that the indole C2–<sup>2</sup>H bond makes an angle of about 5.8° with the normal to the ring bridge.

in membrane-spanning peptides, which circumvents a need to make assumptions concerning constraints due to backbone-folding.

We will discuss first the ring geometry and <sup>2</sup>H spectral assignments, then considerations of the backbone-independent analysis and the descriptions of ring motion, and then a linkage of the “free-ring” analysis to specific backbone models. Finally, we will consider the general implications for tryptophan molecular modeling.

**Ring Geometry and Spectral Assignments.** Early attempts to assign the <sup>2</sup>H NMR spectra for tryptophans in gA relied heavily on molecular modeling. Whereas some modeling and refinement schemes permit the indole rings (whether intentionally or not) to deviate from a strictly planar geometry, microwave spectroscopy<sup>41</sup> and theoretical considerations (Table 3) dictate a planar fused ring system. While the six-membered ring does seem virtually symmetric in shape, the orientation of the C2–<sup>2</sup>H bond was found to be a key parameter for the successful computation of <sup>2</sup>H NMR spectra throughout ring rotational space. We found the bond direction to differ from the normal to the ring bridge by  $6.2^\circ \pm 1.0^\circ$  experimentally, which should be compared with  $5.8^\circ (\pm \text{about } 0.1^\circ \text{ or less})$  from ab initio calculations using several basis sets.

We note that similar indole ring geometries, but without emphasis on the hydrogen positions, have been reported from calculations that compared the ground state properties with several excited states of indole<sup>42,43</sup> and from small-molecule X-ray crystallography of acetyl-tryptophan-methylamide.<sup>39,40</sup> The coordinates for non-hydrogen atoms from two crystal structures<sup>39,40</sup> differ by an rmsd of 0.028 Å. The averaged coordinates for non-hydrogen atoms from these structures<sup>39,40</sup> agree somewhat better (Figure 8) with the ab initio results than with a simple symmetric indole ring. When the X-ray hydrogen (*x*, *y*) coordinates are considered, this averaged crystal structure predicts an “in-plane” angle of 5.5° between the critical C2–<sup>2</sup>H bond and the normal to the bridge. The calculation that led to our early incorrect assignment of the *d*<sub>5</sub>-Trp-9 spectrum of gA<sup>16</sup> is reproducible with a symmetric indole and now is attributed almost entirely to a wrong assumption about the C2–<sup>2</sup>H bond orientation. In retrospect, a previously observed

pattern of deviations of predicted indole C–<sup>2</sup>H bond orientation angles, which suggested “a systematic discrepancy in the data set or the model”,<sup>16</sup> is now clarified.

With the experimental approach to specific <sup>2</sup>H-labeling at the indole C2 and C5 positions, the potential uncertainties associated with molecular modeling become greatly reduced. The combined ab initio calculations, modeling, and partial specific labeling results lend a high level of confidence to the spectral assignments and to the very close alignment of the principal V<sub>zz</sub> C–<sup>2</sup>H tensor components with the bond directions corresponding to the coordinates in Table 3. Furthermore, the specific labeling allowed clarification of the closely similar C2–<sup>2</sup>H and C6–<sup>2</sup>H resonances for Trp-11 (Figure 2), which had been difficult to distinguish by modeling.

We note also that the ab initio calculations were performed on 3-methyl indole. The geometric conclusions therefore should be applicable to 3-substituted indoles generally and not just those in peptides or proteins. As Supporting Information, we provide coordinates for *N*-acetyl-tryptophan-methylamide from a B3-LYP/6-311G\*\* calculation.

**Backbone-Independent Analysis with Respect to the Membrane Normal.** Several closely related models for gramicidin channels in SDS micelles or DMPC bilayer membranes have been determined by NMR methods<sup>22,37,38</sup> While by and large similar, the different models vary somewhat in the precise orientations of the Trp C<sub>α</sub>–C<sub>β</sub> bonds with respect to the bilayer normal (or helix axis) from model to model or even from Trp to Trp within one model (see below). For this reason, direct comparisons of the indole ring orientations from different tryptophans, with respect to the lipid bilayer, are more easily accomplished using a backbone-independent or “free-ring” approach (see Materials and Methods). The two angles ρ<sub>1</sub> and ρ<sub>2</sub> (Figure 1) are sufficient to specify the indole ring orientation with respect to H<sub>o</sub>, while the dynamics were estimated with an overall S<sub>zz</sub> for the ring. When four quadrupolar splittings are observed and assigned and three parameters (ρ<sub>1</sub>, ρ<sub>2</sub>, and S<sub>zz</sub>) are fit to the data, the system is “overdetermined” by one measurement. When applied to gA channels, the method reveals Trp indole ring orientations (Figure 7) that are independent of assumptions concerning the backbone helical model. We note that Separovic and co-workers deduced similar orientations for tryptophans 9, 11, and 13 based on analysis of the <sup>13</sup>C shielding tensor at C4 of indole.<sup>20</sup>

**Backbone Connections for Three Related Models.** When an indole ring from Figure 7 is connected to a backbone model which defines a particular C<sub>α</sub>–C<sub>β</sub> bond direction for the Trp under consideration, it is known that up to eight sets of side-chain (χ<sub>1</sub>, χ<sub>2</sub>) torsion angles are consistent with a particular ring orientation with respect to the membrane normal.<sup>15,17</sup> Four of the eight (χ<sub>1</sub>, χ<sub>2</sub>) combinations would direct the indole NH bond unrealistically toward the bilayer center and can thereby be excluded from consideration.<sup>15–17</sup> Among the remaining pairs of (χ<sub>1</sub>, χ<sub>2</sub>) that orient the indole NH favorably for hydrogen bonding at the membrane/water interface, some may be excluded based on steric interference,<sup>17</sup> while one or more sets may remain as viable solutions. Using closely related models for the β<sup>6,3</sup>-helical backbone of the gA channel, unique regions of (χ<sub>1</sub>, χ<sub>2</sub>) space have been proposed for tryptophans 11, 13, and 15,<sup>16,17,37,38</sup> while two alternative solutions have been proposed for Trp-9 of gA in DMPC. Trp-9 is thought to be either

(42) Slater, L.; Callis, P. J. *Phys. Chem.* **1995**, *99*, 8572–8581.

(43) Serrano-Andres, L.; Roos, B. O. *J. Am. Chem. Soc.* **1996**, *118*, 185–195.



approximately parallel to Trp-11, “sandwiching” Leu-10 between these two indoles,<sup>38,16,37</sup> or “stacked” approximately parallel to Trp-15.<sup>17,22</sup> The matter has remained without a unanimous resolution, despite the fact that the Trp-9/Leu-10/Trp-11 side-chain “sandwich” arrangement is definitive in SDS micelles<sup>37,38</sup> and, in DMPC, is supported by acylation studies<sup>19,26</sup> and by mutational experiments at residue 10.<sup>5</sup> Recent molecular dynamics simulations<sup>44</sup> also support the Trp-9/Leu-10/Trp-11 “sandwich” as representing the major Trp-9 side-chain conformer in DMPC bilayer membranes.

Of importance for protein structure modeling are the questions: How do the indole ring orientations from Figure 7 correspond to  $\chi_1$  and  $\chi_2$  angles? To what extent do these angles vary among different backbone models or even between different sequence positions within one model? We approached these questions using the backbones of models IMAG<sup>22</sup> and IJNO<sup>37</sup> from the Protein Data Bank and our refinement<sup>21</sup> of the original Arseniev  $\beta^{6.3}$ -helical model.<sup>38</sup> We used the indole ring coordinates from Table 3 to replace the Trps in each model, rotated the rings through all possible  $\chi_1$  and  $\chi_2$  angles, and tested each of these ( $3 \times 4$ ) Trps against a common data set of quadrupolar splittings (chosen from Table 2). Each Trp in each model yielded a set of eight possible ( $\chi_1, \chi_2$ ) solutions whose rmsd values closely match those of the corresponding ( $\rho_1, \rho_2$ ) minima in the contour plots of Figure 5. When particular ( $\chi_1, \chi_2$ ) solutions for the different models were compared, the local “spread” in ( $\chi_1, \chi_2$ ) values matching a particular ( $\rho_1, \rho_2$ ) solution was about  $\pm 4^\circ$  in  $\chi_1$  and  $\pm 8^\circ$  in  $\chi_2$ . The variations in helical structure from position to position within each model also correspond to variations in  $\chi_1$  and  $\chi_2$  of about  $\pm 4^\circ$  and  $\pm 8^\circ$ , respectively. Interestingly, this seems to match the respective variations among different gramicidin models. For the backbone of model IJNO, our results correspond to ( $\chi_1, \chi_2$ ) of (189, 66), (288, 301), (286, 286), and (309, 269) for tryptophans 9, 11, 13, and 15, respectively. (These results may be compared to those in Protein Data Bank file IJNO, when Trps 9 and 11 “sandwich” Leu-10: ( $\chi_1, \chi_2$ ) of (182, 86), (300, 301), (296, 274), and (302, 281) for tryptophans 9, 11, 13, and 15 from 2-D NMR of gA in SDS micelles.<sup>37</sup>)

**Indole Ring Motion.** The Trp indole orientations shown in Figure 7 correspond to time-averaged orientations. For <sup>2</sup>H NMR spectroscopy, the availability of four geometrically distinct labels on a single indole ring is sufficient to determine the two geometric parameters in addition to a principal order parameter  $S_{zz}$ . (The experimental information content, with four unique C-<sup>2</sup>H tensors, is intrinsically higher than for a single <sup>15</sup>N or <sup>19</sup>F tensor. Additionally, <sup>19</sup>F will change the ring dipole and could perturb the ring orientation. In principle, multiple <sup>13</sup>C labels could be used.<sup>20</sup>) For each indole ring in gA,  $S_{zz}$  approaches that of the backbone atoms, meaning that the rings are only marginally more mobile than the peptide backbone planes. The relative lack of ring motion should be due primarily to Trp/lipid interactions as well as *intramolecular* indole/side chain or indole/backbone interactions. Changing the identity of one or several neighboring Leu side chains does alter the properties of the tryptophans in gA and in some cases even induces backbone-folding polymorphism.<sup>5,45</sup> By contrast, several lines

of evidence indicate that intermolecular interactions between gA molecules are not dictating the properties of the Trp rings in the oriented gA/DMPC samples: (i) changing the peptide/lipid ratio from 1:10 to 1:40 does not influence the quadrupolar splittings; (ii) the narrow lines in spectra when samples are oriented at  $\beta = 90^\circ$  indicate rapid rotational diffusion of gramicidin dimers; (iii) X-ray diffraction measurements<sup>46</sup> show no evidence for lateral association of gA channels in oriented dilauroylphosphatidylcholine bilayers at gA/lipid molar ratios of 1:10.

In a previous study,<sup>17</sup> anisotropic motion parameters were estimated for Trp indole rings in gA, based upon spectral data from fast-frozen samples and a reasonable assumption that  $\chi_2$  is the principal axis for ring motion. (We also have observed a greater model- and sequence position-dependent “spread” in  $\chi_2$  values than in  $\chi_1$  values; see above.) Attempts to describe anisotropic motion, nevertheless, raise several questions, including: Why do the apparent motion parameters ( $S_{zz}$ ) seem to approach 1.0 for some ring positions,<sup>17</sup> implying that some side-chain atoms experience *less* motional averaging than either the gA backbone atoms or the surrounding lipid headgroups? What parameters were assumed for the indole ring geometry (cf., Results above)? Was the freezing process “fast” enough to preclude temperature-induced molecular rearrangements, including those associated with possible lipid phase polymorphism? (For example, Grage et al. have deduced from <sup>19</sup>F NMR a difference of  $\sim 20^\circ$  in the indole alignment of F-Trp between gel-state and fluid-phase lipids.<sup>6</sup>)

In the present study, we have insufficient information to estimate anisotropic parameters for ring motion, and so we are unable to address the preceding questions. Also from <sup>19</sup>F NMR data of fluorinated Trp-13 and Trp-15 in gA, it was concluded<sup>6</sup> that “all three <sup>19</sup>F CSA tensor values are affected by librational motion in a complex way,” implying that the analysis of anisotropic motion would be difficult. Similar to the published <sup>19</sup>F and <sup>13</sup>C tensor determinations with the gA Trps, our analysis of four C-<sup>2</sup>H tensors on each indole ring seems compatible with an estimation of overall motional averaging, as reflected by  $S_{zz}$  and the concomitant reduction in “effective” QCC for the whole ring. These estimates (Table 4) imply that the “outer” indole rings of Trp-13 and Trp-15 experience only slightly greater motion ( $S_{zz} \approx 0.86$ ) than do backbone groups ( $S_{zz} \approx 0.93$ ), while the “inner” rings of Trp-9 and Trp-11 are characterized by again only slightly greater motional freedom ( $S_{zz} \approx 0.80$ ). We note that the Trp side chains are attached to a rather *rigid* backbone within a highly *mobile* lipid environment and that the comparative extent of ring motion is quite small. Other interactions between side chains and lipids (if observed in other systems) could further increase the side-chain motions (since lipid order parameters are much lower than 0.8).

**Tryptophan Molecular Modeling in Membrane Proteins.** The method of partial <sup>2</sup>H/<sup>1</sup>H exchange at C2 and C5 for spectral assignment combined with the ab initio coordinates of the indole ring (Table 3) will be useful for the refinement and modeling of tryptophans in protein structures generally and particularly for solid-state NMR investigations of labeled membrane proteins, where the whole-molecule orientation may be known with respect to the magnetic field. Even with the “well understood”

(44) Allen, T. W.; Andersen, O. S.; Roux, B. *J. Am. Chem. Soc.* **2003**, *125*, 9868–9877.

(45) Jude, A. R.; Greathouse, D. V.; Koeppe, R. E., II; Providence, L. L.; Andersen, O. S. *Biochemistry* **1999**, *38*, 1030–1039.

(46) Harroun, T. A.; Heller, W. T.; Weiss, T. M.; Yang, L.; Huang, H. W. *Biophys. J.* **1999**, *76*, 937–945.

gramicidin channel system, for which the ring motions are relatively small and the  $^2\text{H}$  quadrupolar splittings well resolved and easily measurable,<sup>17</sup> we have seen that imprecision in the ring geometry can lead to imprecision concerning the spectral assignments.<sup>16</sup> While the refined indole ring geometry discussed here has particular importance for  $^2\text{H}$  NMR spectroscopy (especially for the C2-deuteron), similar geometric considerations are also important for the analysis of  $^{13}\text{C}$ ,  $^{15}\text{N}$  and  $^{19}\text{F}$  NMR spectra. The refined indole ring average orientations (Figure 7), in turn, will influence the ongoing assessments of the indole's dipolar contribution to the energy profiles for ion movement through gA channels and derivatives.<sup>18,47–49</sup>

These results show yet again that the gramicidin channel is a “model” model system, which has been instrumental in establishing important general principles in areas such as: permeation theory,<sup>50–52</sup> single-file ion/water flux coupling,<sup>53</sup> bilayer/channel coupling,<sup>54</sup> dipolar modulation of ion conduc-

tance,<sup>48,49,55,56</sup> sequence-dependent folding,<sup>57,58</sup> Trp anchoring at the membrane/water interface,<sup>14</sup> and voltage-dependent gating.<sup>59</sup> To this list we now add the experimental confirmation of ab initio indole ring geometry as yet another contribution from gramicidin channel research to fundamental knowledge.

**Acknowledgment.** This work was supported in part by NSF Grant MCB 9816063 and NIH Grant RR 15569. We thank Prof. Olaf Andersen from the Weill Medical College of Cornell University for helpful discussions. We also thank two perceptive referees for useful suggestions.

**Supporting Information Available:** B3-LYP/6-311G\*\* ab initio coordinates for *N*-acetyl-tryptophan-methylamide. This material is available free of charge via the Internet at <http://pubs.acs.org>.

JA035052D

- (47) Hu, W.; Cross, T. A. *Biochemistry* **1995**, *34*, 14147–14155.  
(48) Andersen, O. S.; Greathouse, D. V.; Providence, L. L.; Becker, M. D.; Koeppel, R. E., II. *J. Am. Chem. Soc.* **1998**, *120*, 5142–5146.  
(49) Busath, D. D.; Thulin, C. D.; Hendershot, R. W.; Phillips, L. R.; Maughan, P.; Cole, C. D.; Bingham, N. C.; Morrison, S.; Baird, L. C.; Hendershot, R. J.; Cotten, M.; Cross, T. A. *Biophys. J.* **1998**, *75*, 2830–2844.  
(50) Luger, P. *Biochim. Biophys. Acta* **1973**, *311*, 423–441.  
(51) Levitt, D. G. *Biophys. J.* **1978**, *22*, 209–219.  
(52) MacKay, D. H. J.; Berens, P. H.; Wilson, K. R.; Hagler, A. T. *Biophys. J.* **1984**, *46*, 229–248.  
(53) Rosenberg, P. A.; Finkelstein, A. J. *Gen. Physiol.* **1978**, *72*, 327–340.

- (54) Huang, H. W. *Biophys. J.* **1986**, *50*, 1061–1070.  
(55) Mazet, J. L.; Andersen, O. S.; Koeppel, R. E., II. *Biophys. J.* **1984**, *45*, 263–276.  
(56) Koeppel, R. E., II; Mazet, J.-L.; Andersen, O. S. *Biochemistry* **1990**, *29*, 512–520.  
(57) Durkin, J. T.; Providence, L. L.; Koeppel, R. E., II; Andersen, O. S. *Biophys. J.* **1992**, *62*, 145–159.  
(58) Salom, D.; Perez-Paya, E.; Pascal, J.; Abad, C. *Biochemistry* **1998**, *37*, 14279–14291.  
(59) Oiki, S.; Koeppel, R. E., II; Andersen, O. S. *Proc. Natl. Acad. Sci. U.S.A.* **1995**, *92*, 2121–2125.